Numerical evaluation of the carbonation effect on the seismic vulnerability of a RC plane frame

Vincenzo Rinaldi[a], Martina Sciomenta[a], Michele Angiolilli[a], Massimo Fragiacomo[a]
[a] *Dipartimento di Ingegneria Civile, Edile e Architettura, Via Giovanni Gronchi 18, 67100, L'Aquila, Italy*

Keywords: Reinforced structures; Seismic Hazard; Durability; Carbonation effect; Non-linear analysis

ABSTRACT
Corrosion in reinforced concrete structures is a natural process which represents a major source of deterioration in buildings exposed to different environmental conditions. There are a significant number of existing buildings that suffer from material ageing and deterioration, especially those one built before the '90s. In the last decades, researchers have clearly demonstrated that corrosion may lead to a strong reduction in the mechanical properties of both the component materials (steel and concrete) in terms of strength, stiffness and ductility as well. For these reasons, corrosion should be considered both when assessing the seismic vulnerability of existing R.C. buildings and when designing new buildings according to the current standards.
In this paper, a probabilistic approach is proposed to assess the influence of the carbonation effect on the non-linear structural response of a R.C. structure by computing the variation of the mechanical properties of the materials according to formulations found in literature. In particular, fragility curves are obtained for a reinforced concrete plane frame, designed according to the Italian Code (NTC18), by varying the ageing time of the structure under certain constant environmental conditions. Furthermore, a comparison among different design details adopted for the R.C. section and their effects on the fragility of the frame has been carried out. For this purpose, Pushover analyses and Incremental Dynamic Analyses (IDA), the latter performed using natural spectrum-compatible seismic records, have been carried out by using the OpenSees framework.
Results show that the adoption of suitable design details is crucial to limit the reduction in seismic vulnerability of R.C. frames due to carbonation of concrete and corrosion of reinforcement.

1 INTRODUCTION

Since the use of reinforced concrete in construction is a relatively new innovation, 70 years old reinforced concrete structures have only recently begun to show the intrinsic defects related to their durability. Nowadays structural durability is becoming crucial in structural design due to the possible sudden collapse of some structures occurred in different places of the world.

The corrosion effect in reinforced concrete structures is influenced by several variables. Figure 1 summarizes a sample of 10000 real cases collected by Patterson (1984) (Pedeferri 1985) where the causes of corrosion were investigated. It is evident that in 88% of the cases, corrosion is due to errors in design or construction.

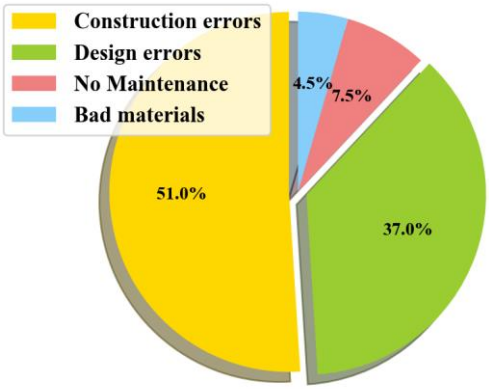

Figure 1. Corrosion causes by Patterson (Pedeferri 1985).

In cities where the concentration of CO_2 is in continuous growth (Mitchell et al. 2018), the carbonation phenomenon is the most common type of reinforced concrete degradation.

The above mentioned effect leads to a reduction in the service life of the structures due to a decrease of the rebars section and ductility

(Imperatore and Rinaldi Z. 2008), crack formation, and bond strength degradation (Al-Salaimani et al. 1990, Bossio et al. 2015).

This paper investigates the effect of carbonation on the seismic vulnerability of a 2D bare reinforced concrete frame placed at the ground floor, and designed with the current Italian building code (M. D. I. e dei trasporti 2018-2019).

2 CARBONATION EFFECT

The carbonation effect depends upon the presence of CO_2 in the environment.

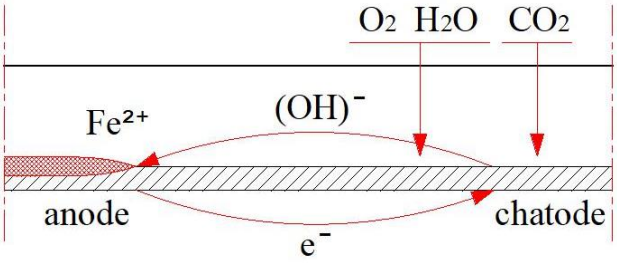

Figure 2. Corrosion induced by carbonation.

Carbonation is a chemical reaction in which carbon dioxide (present in the air), CO_2, reacts with calcium hydroxide, $Ca(OH)_2$, to produce calcium carbonate, $CaCO_3$, and water, H_2O. This reaction reduces the pH of the concrete (originally about 13) to a value between 7 and 9. Normally, a markedly basic environment is created within the cement conglomerate due to the hydration reactions of the binder. This condition promotes the formation of a very thin film of oxides on the steel rebars that protects the metal from further oxidative attacks: this phenomenon is called iron passivation. When the carbonation front reaches the reinforcing steel surface, the passive layer is neutralized and, in the presence of oxygen and water, corrosion may occurs. Corrosion products leads to rebar swelling, which induces tensile stresses in the cover that may breaks the cover itself, leading to an acceleration in the corrosion process.

Therefore, the carbonation effect is an important phenomenon that changes the mechanical and geometrical proprieties of concrete and reinforcing steel in RC structures. For these reasons, the carbonation phenomenon may be a serious issue especially for existing buildings realized before the ‘90s when the corrosion effect was not considered in design.

2.1 Concrete

The swelling of the rebar due to carbonation is a phenomenon difficult to describe since it depends upon several variables including w/c ratio, cement type, the curing type and environmental temperature. Many formulations have been proposed to define the expansion of the carbonation front. The most widespread formulations are based on the Fick’s law, but, for new structures, it is difficult to find the value of the diffusion factor (mm/year$^{0.5}$). In this paper, to predict the evolution of the carbonation depth over time *x(t)* [mm], the Duval’s formulation (Duval 1992) was adopted:

$$x(t) = \sqrt{365 \cdot t} \cdot (1 / (2.1 \cdot \sqrt{f_{c28}}) - 0.06) \quad (1)$$

where *t* [years] is the time of exposure and f_{c28} [MPa] is the mean cylindrical concrete compressive strength after 28 days from the concrete placement.

Another aspect related to the carbonation depth in concrete is the increase in strength and elastic modulus due to a reduction in the porosity as demonstrated by Cheng-Feng and Jing-Wen (Cheng-Feng and Jing-Wen 2005). However, crack formation leads to damage (cracking and spalling) of the cover which undo that effect.

2.2 Reinforcing steel

The carbonation phenomenon does not cause problems to the concrete itself but rather to the reinforcing bars. By changing the protective conditions around the steel rebar allows the beginning of the corrosion, which modifies the mechanical and geometrical proprieties of reinforcing bars over time. Corrosion of steel rebars depends on many variables such as: concrete resistivity, relative humidity, chloride content, distribution, depth and width of the cracks (Bertolini et al. 2013). The carbonation attack, differentially from the chloride attack, is related with a uniform reduction in the bar diameter along the length of the reinforcement.

Figure 3 (Tuutti 1982) depicts the degree of corrosion of steel rebars due to carbonation or chloride ion penetration over time. The first phase is defined as initiation period (t_i) which is the time required by the carbonation front to reach the steel rebars. The second phase is named propagation period (t_p) which is the time necessary to reach a certain limit condition.

In literature the are many formulations that can be used to calculate the loss of material due to the corrosion (propagation period). Vu and Stewart (Vu and Stewart 2000) proposed the following empirical formulation valid for a RH of the

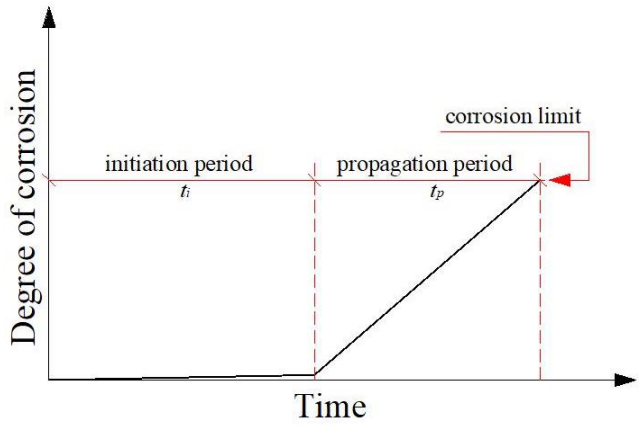

Figure 3. Degree of corrosion (Tuutti 1982) vs time.

environment equal to 75% and a temperature of 20°C:

$$i(t_i) = [37.8 \cdot (1 - w/c)^{-1.64}] / C \quad (2)$$

$$i_{prop}(t_p) = 0.85 \cdot i(t_i) \cdot t_p^{-0.29} \quad (3)$$

$$V_{corr}(t_p) = 0.0116 \cdot i_{prop}(t_p) \quad (4)$$

where $i(t_i)$ [μA/cm^2] is the rate of corrosion at the beginning of the propagation period, *w/c* is the water/cement ratio and *C* [mm] is the cover thickness. $i_{prop}(t_p)$ [μA/cm^2] is the corrosion current density in the propagation period t_p [year]. V_{corr} [mm/years] is the corrosion rate calculated according the Faraday's law for iron.

Assuming a uniform corrosion rate during the propagation period (Figure 4), the progressive loss of rebar section $P(t_p)$ can be expressed as:

$$P(t_p) = V_{corr}(t_p) \cdot t_p \quad (5)$$

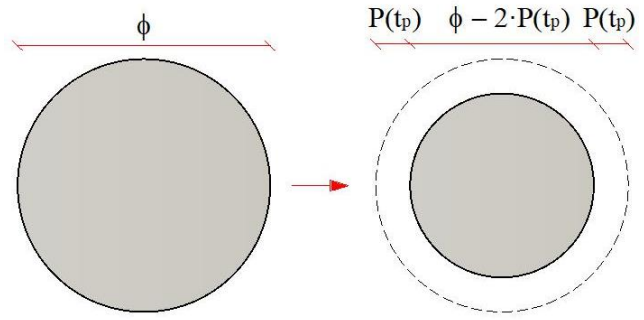

Figure 4. Uniform corrosion.

2.3 Service Life

The service life of a structure defines the period during which the structure has to satisfy the performance criteria. By monitoring the material degradation it may be possible to define the limit state of a concrete structure. According to Tuutti (Tuutti 1982) the service life is the sum of the initiation and the propagation periods. Whilst the value of t_i is relatively easy to assess for existing buildings and more complex for new structures, the calculation of t_p is complex for both cases. Andrade et al. (Andrade et al. 1993) suggests that if the cracks width exceeds the value of 0.3≈0.5 mm, the structure cannot be repaired and therefore that value could be used as a limit state. To evaluate the crack width w_{cr} [mm], Molina et al. (Molina et al. 1993) proposed an empirical formulation:

$$w_{cr}(t_p) = 2\pi \cdot (\nu_{rs} - 1) \cdot P(t_p) \quad (6)$$

where $P(t_p)$ is the corrosion penetration given by Equation 5 and v_{rs} is the ratio between the volumetric expansion of the oxides and the virgin material (assumed equal to 2.0). Once the corrosion penetration function is defined, the propagation period can be calculated as the time needed to achieve a certain crack width.

3 CASE OF STUDY

One of the most common residential building archetype in Italy is a reinforced concrete moment-resisting frame characterized by a ground floor without (or with only few) partitions for practical/architectonic considerations (Figure 5). This type of structure may potentially suffer from significant seismic issues especially if capacity design was not carried out like in the buildings designed before the '90s. In order to investigate how the durability can influence the seismic vulnerability, a 2D reinforced frame of three storey and two bays has been analysed.


Figure 5. Example of a typical RC building with no partitions at the ground floor damaged by the L'Aquila earthquake (2009).

The structure has been designed according to the recent Italian Design Code (M. D. I. e dei trasporti 2018). The loads were evaluated considering a residential building (class use II)

and a cast in-situ RC floor. The service life of the structure was assumed equal to 50 years.

The first and the second floors has been considered as exposed to inner environmental conditions whereas the ground floor was regarded as exposed to outdoor conditions. Table 1 lists the gravity loads per unit floor. A 5m tributary width was assumed for the frame.

Table 1. Gravity loads.

Storey	G_{k1} [kN/m^2]	G_{k2} [kN/m^2]	Q_{k1} [kN/m^2]
1	3.2	2.5	2.0
2	3.2	2.5	2.0
3	3.2	1.5	2.1-0.5

The structure in Figure 6 was designed using a linear-static analysis, taking into account gravity and horizontal (earthquake only) loads. The structure is located in L'Aquila on a soil site class type C and topographic category T1 with a PGA= 0.347g for the Significant Damage Limit State (T_r = 450 years).

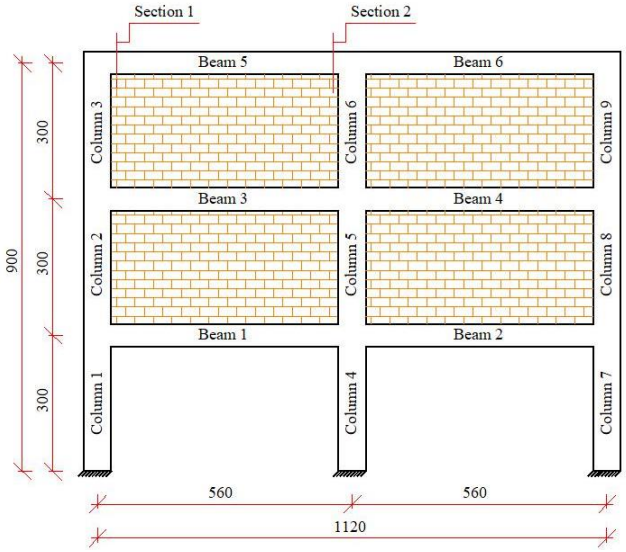

Figure 6. 2D reinforced concrete frame.

The 2D frame was designed in ductility class B (moderate), assuming a behaviour factor *q* equal to 2.76, according to NTC18, and considering the structure as irregular due to the mass distribution. The NTC18 and UNI EN 206:2016 (UNI EN 2006) require compliance with specific limits of water-cement (*w/c*) ratio, concrete class strength and thickness of the concrete cover to prevent corrosion problems and to avoid the concrete degradation. Since the exposure class is regarded as "ordinary condition" in the ground floor (XC3), a concrete class C30/37 (f_{cm28}=30+8=38MPa) was chosen for the entire frame, with *w/c* equal to 0.45 and cover thickness equal to 35mm.

Two different structures, Model A and Model B, were considered: section geometry, number and type of reinforcing bars were the same, but the thickness of the concrete cover, assumed uniform for all sections of each structural elements (beams and columns), was different.

In Model A, the nominal cover thickness (Figure 7) of 35mm (25mm+10mm) was assumed in accordance with the durability rules of the Italian code. In Model B, a reduced cover thickness of 15mm was assumed, representing the case of a wrong construction detail.

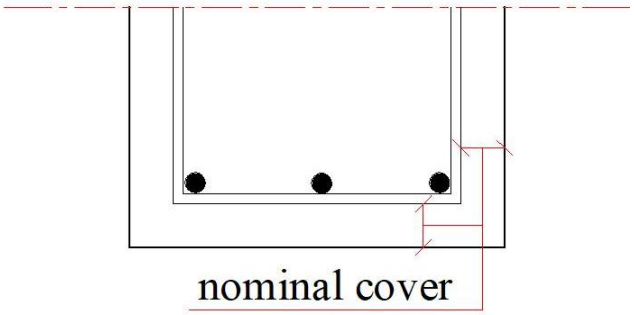

Figure 7. Nominal cover.

It was assumed that only the ground storey columns and the first storey beams underwent the carbonation phenomenon that leads to a reduction of the reinforcing bar area and the spalling of the concrete cover being exposed to outdoor conditions. No carbonation was assumed to take place in indoor conditions because the relative humidity is low (Bertonili et al. 2013). The base columns were assumed to be subjected to carbonation corrosion on each side of the cross section, whilst the beams of the first level were considers subjected to corrosion on the lateral and bottom side only.

3.1 Structural details according to the Italian Code

According to the NTC18, the structure was designed using capacity design to avoid brittle failure such as shear in beams and columns and joint failure. The only possible allowed collapse mechanism was flexure (ductile mechanism) at the ends of the beams and at the foundation-column connections. To avoid an overdesign, ϕ14 and ϕ18 were used for the longitudinal rebars respectively for beams and columns, and ϕ8 were used for the transversal reinforcement. Tables 2, 3 and 4 summarize the number and type of reinforcing bars in the dissipative zones (steel rebars with an asterisk "*" were subjected to corrosion).

Table 2. Structural elements details - section 1.

Element	Top	Bottom
Beam 1 [30x50] st.1ϕ8@10cm*	5ϕ14	4ϕ14*
Beam 2 [30x50] st.1ϕ8@10cm*	6ϕ14	6ϕ14*
Beam 3 [30x50] st.1ϕ8@10cm	5ϕ14	3ϕ14

Beam 4 [30x50] st.1ϕ8@10cm	5ϕ14	6ϕ14
Beam 5 [30x50] st.1ϕ8@10cm	3ϕ14	3ϕ14
Beam 6 [30x50] st.1ϕ8@10cm	4ϕ14	4ϕ14

Table 3. Structural elements details - section 2.

Element	Top	Bottom
Beam 1 [30x50] st.1ϕ8@10cm*	6ϕ14	6ϕ14*
Beam 2 [30x50] st.1ϕ8@10cm*	5ϕ14	4ϕ14*
Beam 3 [30x50] st.1ϕ8@10cm	5ϕ14	6ϕ14
Beam 4 [30x50] st.1ϕ8@10cm	5ϕ14	3ϕ14
Beam 5 [30x50] st.1ϕ8@10cm	4ϕ14	4ϕ14
Beam 6 [30x50] st.1ϕ8@10cm	3ϕ14	3ϕ14

Table 4. Structural elements details - section 1 and 2.

Element	Top-Bottom
Column 1 [30x60] st.1ϕ8@10cm*	10ϕ18*
Column 2 [30x60] st.1ϕ8@10cm	10ϕ18
Column 3 [30x60] st.1ϕ8@10cm	10ϕ18
Column 4 [30x60] st.1ϕ8@10 cm*	12ϕ18*
Column 5 [30x60] st.1ϕ8@10cm	12ϕ18
Column 6 [30x60] st.1ϕ8@10cm	10ϕ18
Column 7 [30x60] st.1ϕ8@10 cm*	10ϕ18*
Column 8 [30x60] st.1ϕ8@10cm	10ϕ18
Column 9 [30x60] st.1ϕ8@10cm	10ϕ18

3.2 Numerical model

The OpenSees framework (McKenna 2011) (v. 3.0.3) was used to perform the non-linear analysis of the 2D reinforced concrete frame using the standard library.

The frame was fixed at the base of the columns. The beams were subjected to uniformly distributed gravity loads. The storey masses were lumped at the storeys' nodes. A 5% Rayleigh damping was adopted.

Nonlinear beam-column elements were used to model the RC frame with distributed plasticity. The regions where the development of the plastic hinge may occur were modelled with a fiber sections. The fiber section was used as it allows the user to consider the material proprieties of concrete cover, core concrete and steel rebar.

Beams and columns were modelled using the forceBeamColumn element (beamWithHinges) with six element integration points. This element accounts for linear and P-Δ effect, respectively for beams and columns. The plastic hinges length was assumed equal to the structural element depth and the joint were modelled using rigid links. Cross-sections were modelled by defining geometric and material proprieties. The shear behaviour for beams and columns was governed by a linear elastic relationship characterized by a high stiffness representing a fixed constraint. The constitutive models adopted to define the materials properties were the concrete02 and the steel02. Concrete02 material was used to model the concrete (confined and non-confined) without tensile strength following the Kent-Scott-Park model. The mechanical proprieties adopted in concrete02 were evaluated following the modified Kent-Park law. Steel02, based on Giuffre-Menegotto-Pinto model, was associated to reinforced steel rebars. The design values of the strength properties were used both for concrete and steel.

The FE model did not take into account the effect of bond strength degradation due to corrosion. This effect is rather difficult to model in a one-dimension finite element. Also the possible buckling effect of the longitudinal steel rebars was neglected since the spacing between the stirrups was in agreement with the code limits. A constant and uniform relative humidity (RH) was considered in the environment. This is a common assumption made to simplify the issue of time-dependent corrosion intensity, even though this simplification may result very conservative.

3.2.1 Material properties

The material properties were evaluated at different times starting from the time of concrete placement: 28days, 25years, 50years and 75years, using Equations 1, 2, 3, 4 and 5. The possible presence of a plaster for the elements in contact with the outdoor environment, which may affect the evolution of the carbonation front, was conservatively ignored. The beginning of the propagation period was assumed, conservatively, coincident with the trigger time of carbonation on the outer edge for the specific rebar (stirrups and longitudinal bars).

From the results summarized in Tables 5 and 6 it is evident that if the cover thickness complies with the code requirements, no corrosion occurs for the entire service life and beyond (corrosion would start at 112.81 years after the concrete placement). Therefore, in this case the non-linear response of the RC frame does not change during the entire service life and beyond.

Table 5. Initiation period Model A.

	Stirrups	Longitudinal
s [mm]	35	35+8=43
t_i [year]	112.81	170.28

Table 6. Initiation period Model B.

	Stirrups	Longitudinal
s [mm]	15	15+8=23
t_i [year]	20.72	48.72

Unlike for Model A, in Model B corrosion starts at 20.72 years from construction. The

stirrups were attacked first, followed by the longitudinal rebars. Considering different times in the "lifetime" of the structure (28days, 25years 50years and 75years), Tables 7, 8 and 9 summarize the time propagation period for each rebar size type and the corresponding cross-sections.

Table 7. Model B, cross-sections of the ϕ8 stirrups.

year	t_p [year]	%	mm^2
0.08	0.00	-	50
25	8.56	-9.08	43
50	33.56	-33.10	32
75	58.56	-48.48	25

Table 8. Model B, cross-sections of the ϕ14.

year	t_p [year]	%	mm^2
0.08	0.00	-	154
25	-	-	-
50	11.35	-1.47	152
75	36.35	-1.22	135

Table 9. Model B, cross-sections of the ϕ18.

year	t_p [year]	%	mm^2
0.08	0.00	-	254
25	-	-	-
50	11.35	-1.14	252
75	36.35	-9.54	230

As stated in Section 2.3, the service life depends on the crack's width limit, which has been assumed equal to 0.5mm. The time from the concrete placement leading to a crack width formation of 0.5mm has been evaluated based on the corrosion of the stirrups, since they were the first element to undergo corrosion. This time was estimated with the following Equation:

$$t_n = t_i + 0.5/V_{corr}(t_p) = 20.72 + 1.30 = 22.02 \qquad (7)$$

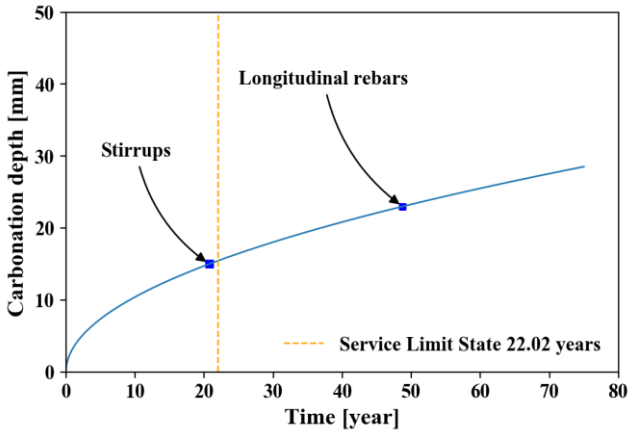

Figure 8. Model B, carbonation depth and Service Limit State.

Figure 8 highlights that Model B had an important reduction in nominal life (about the 56%) and a restoration is required for a cracking width of 0.5mm since only 1.30 years are necessary to reach the corrosion limit of the stirrups.

Without any repair measure, in the following non-linear analyses (except for Model B at 28days) the models were characterized by a section reduction to consider the carbonation effect on the concrete cover.

4 NON LINEAR ANALYSIS

To investigate the non-linear behaviour of the Models A and B, non-linear analysis (push over and incremental dynamic analysis) were carried out. For both models, flexure and shear failure were considered as ultimate limit states according to the Italian Code for the existing buildings.

4.1 Push over analysis

The push over analysis was carried out as displacement control incremental analysis, considering the modal and the masses load distribution. The displacement of the roof was taken as the control point.

4.2 Incremental dynamic analysis

To perform the IDA analyses (Vamvatsikos 2002), a set of seven ground motions records spectrum compatible with the selected site (not scaled), were chosen using REXEL v3.5 (Iervolino et al. 2009) through a disaggregation analysis (M_w 4.5-6.5 and R=25km). Table 10 and Figure 9 summarize the selected records and the correspondent acceleration spectrum. The mean spectrum had lower and upper tolerance equal to respectively 10% and 30% in a period range of 0.15-2.0sec.

Table 10. Selected earthquake records.

TH	Event	Date	PGA [g]
1	Montenegro	24/05/79	0.54
2	Kefallinia	23/03/83	0.31
3	Umb.-Marc.	06/10/97	0.36
4	Umb.-Marc.	03/10/97	0.41
5	Umb.-Marc.	12/10/97	0.38
6	Manesion	07/06/89	0.25
7	Kalamata	15/09/86	0.31

The IDAs were performed by scaling the PGA from 0.0g to 2.0g with an incremental step equal to 0.02g and performing 101 dynamic analyses for each time-history.

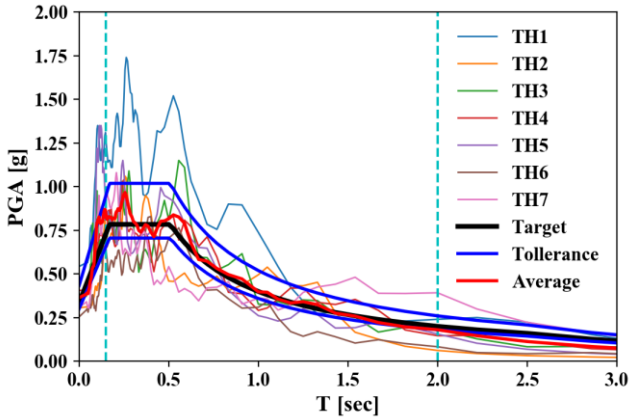

Figure 9. Collection of seven spectrum-compatible accelerograms.

4.3 Comparison of the results

The results of the non-linear analyses (Push-Over and IDA) were summarized in the capacity curves for each model. The IDA curves considered the maximum base-shear vs maximum top displacement for each PGA increment.

In Figure 10 the capacities of Model A are plotted and since the cover thickness complied with current regulations, the load capacity did not change over the years. The collapse observed for the push-over and the IDA analysis was in all cases due to a ductile mechanisms (achievement of the rotation capacity of beams or columns in the critical sections). Furthermore, the maximum base-shear capacity corresponding to the modal push-over paths was 363.61kN, 41.7% greater than the design base-shear calculated according to the Force-Based method. This overstrength was due to the minimum reinforcement requirement prescribed by the Italian Code (concrete type, longitudinal and transversal reinforcement).

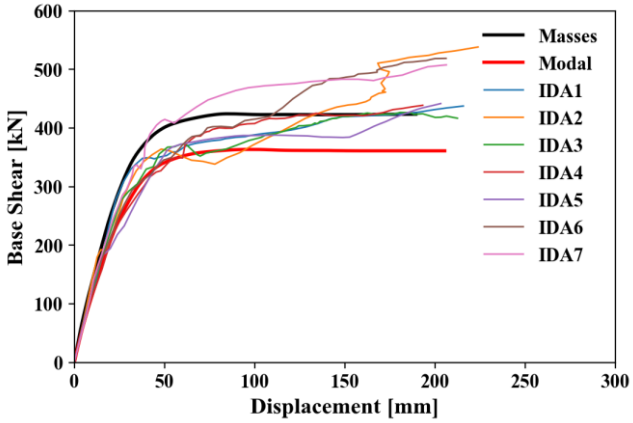

Figure 10. Model A 28days-25-50-75years.

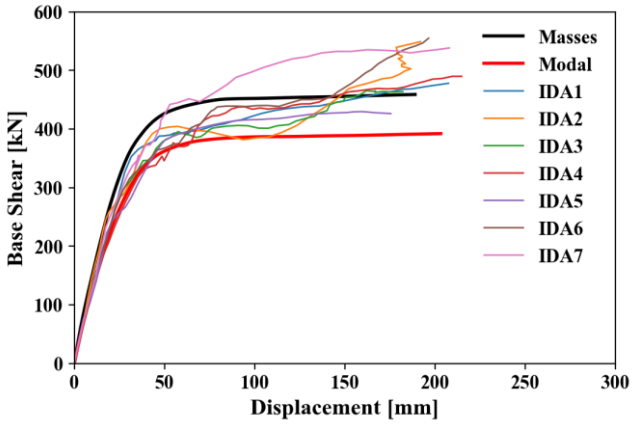

Figure 11. Model B 28days.

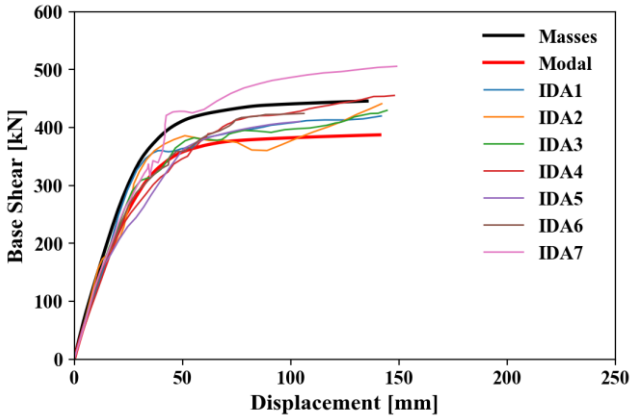

Figure 12. Model B 25years.

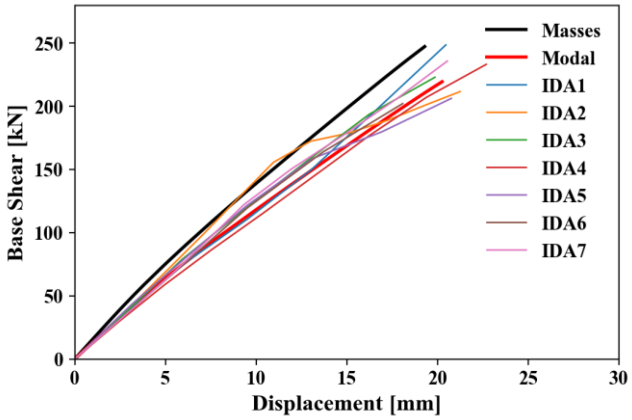

Figure 13. Model B 50years.

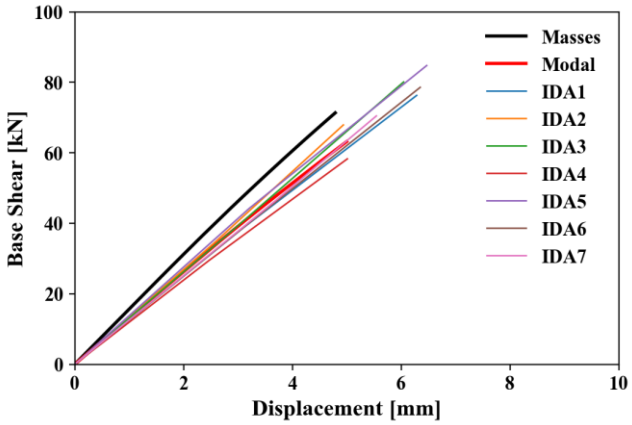

Figure 14. Model B 75years.

Therefore, Model B (Figures 11, 12, 13 and 14) showed a decrease in terms of strength and ductility capacity over the time, especially from 25 to 50 years. Except for the Model at 28day which showed ductile failure, the remaining models had brittle failure (shear collapse for beams 1 and 2). Furthermore, Model B at 28days showed a different global behaviour compared to Model A at the same age. In particular, Model B had a greater global strength and a smaller global displacement capacity due to the increase in the effective depth (3cm) and an increase in the confined concrete sections for all structural elements.

For all models A and B there was a good agreement between the push-over analyses and the IDA analyses, proving the overall accuracy of the push-over results in the two dimensional problems.

Based on the IDA results the vulnerability index for seismic action, ζ_E, was calculated at each life-time for all models according the Italian Code:

$$\zeta_E = \frac{PGA_C}{PGA_D} \tag{8}$$

where PGA_C and PGA_D were respectively the capacity and the demand peak ground acceleration. The results are summarized in Table 11 and plotted in Figure 15.

Table 11. Mean values of the seismic vulnerability indexes.

Model	$PGA_{C,mean}$	PGA_D	ζ_e
A	1.037	0.347	2.99
B 28days	1.034	0.347	2.98
B 25years	0.714	0.347	2.06
B 50years	0.146	0.347	0.42
B 75years	0.043	0.347	0.12

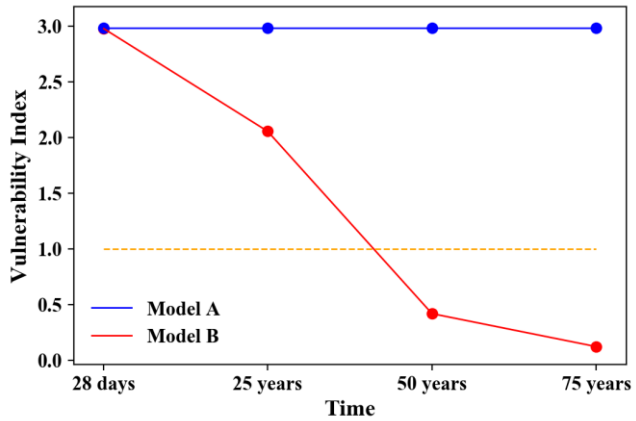

Figure 15. Vulnerability index for Model A and Models B.

Based on the results, Model A had the same vulnerability index for 28 days, 25 years, 50 years and 75 years, and the building complied with the basic principles of the NTC18 according to which a new structure, during the service life, should maintain the same performance level. Conversely, Model B showed a quite constant decrease in the seismic vulnerability over time. As observed at 28 days, Model B had a vulnerability index equal to 2.98. This value also underlines that by complying with the minimum amount of reinforcement required by the Code, the structure has a significant overstrength capacity that can postpone a possible corrosion problems in terms of seismic vulnerability. It should be pointed out, however, that these results may be slightly non-conservative having neglected some phenomena such as the bond degradation due to corrosion, the cover spalling and the rebars buckling.

5 CONCLUSIONS

This paper investigates the effect of the carbonation phenomenon on the seismic vulnerability of a RC plane frame designed according the Italian Building Code 2018. A three-storey, two-bay RC frame structure without partitions at the ground floor was analysed.

Two different models of the same structure were considered: one with a cover thickness complying with regulation requirements (Model A) and another one with an underestimated cover thickness (Model B) which could be due by possible design/construction errors.

The effect of the corrosion was taken into account by considering the rebar cross section reduction and varying the section proprieties in terms of confinement and loss of the cover concrete for the elements in contact with the outer environment.

Through non-linear analysis (Push-Over and Incremental Dynamic Analysis) performed at different points in time and considering the structure degradation during the service life period, Model A showed that the structure was able to maintain the same properties over the time complying with the performance levels required by the Italian Code. Conversely, Model B showed a strong reduction in terms of ductility and strength capacity, making retrofitting measures necessary just after 22 years from the concrete placement.

REFERENCES

Andrade, C., Alonso, C., & Molina, F. J., 1993. Cover cracking as a function of bar corrosion: Part I-Experimental test. *Materials and structures*, **26**(8), 453-464.

Al-Sulaimani, G. J., Kaleemullah, M., & Basunbul, I. A., 1990. Influence of corrosion and cracking on bond behavior and strength of reinforced concrete members. *Structural Journal*, **87**(2), 220-231.

Bossio, A., Monetta, T., Bellucci, F., Lignola, G. P., & Prota, A., 2015. Modeling of concrete cracking due to corrosion process of reinforcement bars. *Cement and concrete research*, 71, 78-92.

Bertolini, L., Elsener, B., Pedeferri, P., Redaelli, E., & Polder, R., 2013. *Corrosion of steel in concrete* (Vol. 392). Weinheim, Germany: Wiley-Vch.

Cheng-Feng, C., & Jing-Wen, C., 2005. Strength and elastic modulus of carbonated concrete. *ACI materials journal*, **102**(5), 315.

Duval, R., 1992. La durabilité des armatures et du béton d'enrobage. *Paris: Pressesde l'École Nationale des Ponts et Chaussées*, 173-225.

Iervolino, I., Galasso, C., & Cosenza, E., 2010. REXEL: computer aided record selection for code-based seismic structural analysis. *Bulletin of Earthquake Engineering*, **8**(2), 339-362.

Imperatore, S., & Rinaldi, Z., 2009. Mechanical behavior of corroded rebars and influence on the structural response of R/C elements. *Proceedings of concrete repair, rehabilitation and retrofitting II. CRC Press, London*, 489-495.

M. D. I. e dei trasporti, 2018. Aggiornamento delle «Norme Tecniche per le Costruzioni». Supplemento ordinario alla "Gazzetta Ufficiale, (42).

M. D. I. e dei trasporti, 2019. Circolare 21 gennaio 2019, n. 7. Istruzioni per l'applicazione dell'«Aggiornamento delle "Norme tecniche per le costruzioni"» di cui al decreto ministeriale 17 gennaio 2018.

McKenna, F., 2011. OpenSees: a framework for earthquake engineering simulation. *Computing in Science & Engineering*, **13**(4), 58-66.

Mitchell, L. E., Lin, J. C., Bowling, D. R., Pataki, D. E., Strong, C., Schauer, A. J., ... & Mallia, D., 2018. Long-term urban carbon dioxide observations reveal spatial and temporal dynamics related to urban characteristics and growth. *Proceedings of the National Academy of Sciences*, **115**(12), 2912-2917.

Molina, F. J., Alonso, C., & Andrade, C., 1993. Cover cracking as a function of rebar corrosion: part 2—numerical model. *Materials and structures*, **26**(9), 532-548.

Pedeferri, P., 1985. La corrosione delle armature nel calcestruzzo. *Convegno sulle opere in calcestruzzo: Durabilità e ripristino*, Milano.

Tuutti, K., 1982. Corrosion of steel in concrete. Cement-och betonginst..

UNI, E., 2006. 206-1: 2006. *Calcestruzzo-Specificazione, prestazione, produzione e conformità*.

Vamvatsikos, D., & Cornell, C. A., 2002. Incremental dynamic analysis. *Earthquake Engineering & Structural Dynamics*, **31**(3), 491-514.

Vu, K. A. T., & Stewart, M. G., 2000. Structural reliability of concrete bridges including improved chloride-induced corrosion models. *Structural safety*, **22**(4), 313-333.